

Second virial coefficients of light nuclear clusters and their chemical freeze-out in nuclear collisions

K. A. Bugaev^{1,2} ^a, O. V. Vitiuk^{2,3}, B. E. Grinyuk¹, V. V. Sagun^{1,4}, N. S. Yakovenko², O. I. Ivanytskyi^{1,4}, G. M. Zinovjev¹, D. B. Blaschke^{5,6,7}, E. G. Nikonov⁸, L. V. Bravina³, E. E. Zabrodin^{3,9}, S. Kabana¹⁰, S. V. Kuleshov¹¹, G. R. Farrar¹², E. S. Zherebtsova^{7,13} and A. V. Taranenko⁷

¹ Bogolyubov Institute for Theoretical Physics, Metrologichna str. 14^B, Kyiv 03680, Ukraine

² Department of Physics, Taras Shevchenko National University of Kyiv, 03022 Kyiv, Ukraine

³ University of Oslo, POB 1048 Blindern, N-0316 Oslo, Norway

⁴ CFisUC, Department of Physics, University of Coimbra, 3004-516 Coimbra, Portugal

⁵ Institute of Theoretical Physics, University of Wrocław, Max Born Pl. 9, 50-204 Wrocław, Poland

⁶ Bogoliubov Laboratory of Theoretical Physics, JINR Dubna, Joliot-Curie Str. 6, 141980 Dubna, Russia

⁷ National Research Nuclear University (MEPhI), Kashirskoe Shosse 31, 115409 Moscow, Russia

⁸ Laboratory for Information Technologies, Joint Institute for Nuclear Research, Dubna 141980, Russia

⁹ Skobel'syn Institute of Nuclear Physics, Moscow State University, 119899 Moscow, Russia

¹⁰ Instituto de Alta Investigación, Universidad de Tarapacá, Casilla 7D, Arica, Chile

¹¹ Departamento de Ciencias Físicas, Universidad Andres Bello, Sazié 2212, Piso 7, Santiago, Chile

¹² Department of Physics, New York University, New York, NY 10003, USA

¹³ Institute for Nuclear Research, Russian Academy of Science, 108840 Moscow, Russia

the date of receipt and acceptance should be inserted later

Abstract. Here we develop a new strategy to analyze the chemical freeze-out of light (anti)nuclei produced in high energy collisions of heavy atomic nuclei within an advanced version of the hadron resonance gas model. It is based on two different, but complementary approaches to model the hard-core repulsion between the light nuclei and hadrons. The first approach is based on an approximate treatment of the equivalent hard-core radius of a roomy nuclear cluster and pions, while the second approach is rigorously derived here using a self-consistent treatment of classical excluded volumes of light (anti)nuclei and hadrons. By construction, in a hadronic medium dominated by pions, both approaches should give the same results. Employing this strategy to the analysis of hadronic and light (anti)nuclei multiplicities measured by ALICE at $\sqrt{s_{NN}} = 2.76$ TeV and by STAR at $\sqrt{s_{NN}} = 200$ GeV, we got rid of the existing ambiguity in the description of light (anti)nuclei data and determined the chemical freeze-out parameters of nuclei with high accuracy and confidence. At ALICE energy the nuclei are frozen prior to the hadrons at the temperature $T = 175.1^{+2.3}_{-3.9}$ MeV, while at STAR energy there is a single freeze-out of hadrons and nuclei at the temperature $T = 167.2 \pm 3.9$ MeV. We argue that the found chemical freeze-out volumes of nuclei can be considered as the volumes of quark-gluon bags that produce the nuclei at the moment of hadronization.

PACS. 25.75.-q Relativistic heavy-ion collisions
05.70.Ce Thermodynamic functions and equations of state
64.30.-t Equations of state of specific substances

1 Introduction

The concept of hard-core repulsion plays an important role in the statistical mechanics of classical systems since, despite its simplicity, it allows one to correctly reproduce the basic properties of real gases at short distances. Its importance in describing the multiplicities of hadrons produced in the central high energy nuclear (A+A) collisions is beyond any doubts. In atomic physics it is clear that the hard core in the intermolecular interaction has its funda-

mental origin in the Pauli exclusion principle and the electron exchange correlations between atoms and molecules (see, e.g., [1] and references therein) which allows one to predict the composition and thermodynamics of inertial fusion plasmas due to the account of the Pauli-blocking effect between atomic clusters [2]. However, the application of the fundamental Pauli principle on the quark level to account for a repulsive hard core in the interaction among hadrons is still in its infancy [3]. The account of the Pauli blocking effect for light clusters in nuclear matter is meanwhile well-elaborated for not too high temperatures

^a e-mail: bugaev@th.physik.uni-frankfurt.de

[4] and for applications to the composition of supernova matter [5,6], where usually excluded volume approaches are applied to account for light cluster abundances [7,8,9]. Within the quantum statistical approach, the second virial coefficient is addressed via a generalized Beth-Uhlenbeck equation of state which accounts for medium effects on the scattering phase shifts among clusters (cluster virial expansion [10]). The latter not only describes systematically the in-medium modification of the hard-core interaction, but ultimately leads to the Mott dissociation of the nuclear clusters due to Pauli blocking. The generalization of this successful quantum statistical approach to the higher temperatures by including all species of a hadron resonance gas and the treatment of repulsive Pauli-blocking effects on the basis of their fermionic quark substructure is a formidable task that has just been started [11]. For the time being, one can already get interesting insights for the discussion of chemical freeze-out (CFO) of light clusters in the QCD phase diagram, in the context of ongoing discussions of the puzzle why these clusters freeze out in ultrarelativistic heavy-ion collisions at CERN and BNL according to predictions of the thermal statistical model at the same high temperature $T_{CFO} \approx 160$ MeV like all the other hadrons while their binding energies are at least an order of magnitude smaller.

This puzzle of the light nuclei production at LHC and RHIC has been discussed in many recent papers [12,13,14,15,16,17,18,19,20,21,22], from both alternative points of view: the coalescence of nucleons (and hyperons, if applicable) in the final state after thermal freezeout of the hadrons on the one hand, and the CFO of the nuclei according to the thermal statistical model together with the other hadronic species directly in the vicinity of the hadronization transition in the QCD phase diagram on the other.

When drawing the lines for the Mott dissociation of light clusters as derived from the quantum statistical model into the QCD phase diagram one observes [23,24] that at the conditions of LHC and STAR experiments the medium modifications for nuclear clusters are not important, so that they can be expected to follow the ordinary thermal statistical model albeit including a hard core repulsion as in free space. Therefore, we devote the present work to extending the concept of hard core repulsion for hadronic systems with nuclear clusters in a thermodynamically consistent way and will apply it to the description of hadron and light cluster yields obtained in these experiments.

The real breakthrough in achieving a very high accuracy in the description of hadronic yields measured from the low AGS BNL collision energy ($\sqrt{s_{NN}} = 2.7$ GeV) to the LHC CERN one ($\sqrt{s_{NN}} = 2.76$ TeV) is related to the hadron resonance gas model (HRGM) with several hard-core radii of hadronic species [25,26,27,28], i.e. with the multicomponent hard-core repulsion. Indeed, using just two extra parameters, the hard-core radii of pions R_π and kaons R_K , in addition to the hard-core radii of baryons R_b and the ones of other mesons R_m which are traditionally employed in the HRGM, it was possible to achieve a very accurate description of all independent hadron multiplic-

ity ratios measured prior to the LHC era with a χ^2/dof which is in the range between 1.15 [26,27,28] and 0.96 [29]. The high accuracy achieved by the HRGM with multicomponent hard-core repulsion allowed us not only to elucidate the characteristics of the CFO of A+A collisions, but also to reveal new irregularities of thermodynamic quantities at the CFO and to formulate new signals of two phase transitions [30,31,32,33,34] which are expected to exist in strongly interacting matter.

We have to remind that traditionally the CFO is defined as the moment after which the inelastic reactions stop to exist, while the evolution of hadronic matter is dominated by elastic reactions towards thermal freeze-out and decays of resonances [35].

However, the multicomponent versions of the HRGM based on the Van der Waals (VdW) approximation to the hard-core repulsion, i.e. which employ the classical second virial coefficients, are rather complicated and they take a lot of CPU time, since for N different hard-core radii for each iteration of the fitting process of experimental data one has to solve the system of $N + 1$ transcendental equations which involve hundreds of double integrals [25,26,27,28,29]. Therefore, the application of the multicomponent HRGM based on VdW approximation to cases of $N \gg 1$ is rather problematic. Fortunately, an entirely new and efficient approach to treat the multicomponent hard-core repulsion for large values of N was invented in Ref. [36]. This novel approach based on the induced surface tension concept has two important advantages over the other multicomponent versions of the HRGM: first, the number of equations to be solved is always two and it does not depend on N and, second, it allows one to go beyond the VdW approximation [37,38,39,40]. Note that the classical virial coefficients are traditionally denoted as the excluded volumes (per particle).

Despite the great achievements of the HRGM one important problem of the CFO was not resolved until recently. It is the CFO puzzle of light (anti)nuclei yields measured by the STAR RHIC collaboration in Au+Au central collisions [42,43,44] at the center-of-mass collision energy $\sqrt{s_{NN}} = 200$ GeV and the ones obtained recently by the ALICE CERN collaboration in Pb+Pb collisions at the center-of-mass collision energy $\sqrt{s_{NN}} = 2.76$ TeV [45,46,47].

There are many important aspects of the CFO puzzle of light (anti)nuclei yields [19,21,22,49,50,57,58,59,60,61,62] measured in A+A collisions, but in our opinion the central one, is the value of their CFO temperature T_A . This is so, since without the reliable knowledge of their CFO temperature T_A one cannot formulate a physically adequate model for the production of deuterons (d), helium-3 (${}^3\text{He}$), helium-4 (${}^4\text{He}$) and hyper-triton (${}^3_\Lambda\text{H}$) and their antiparticles in A+A collisions and a model of their thermalization as well. Other approaches in the literature which describe the production of nuclei in heavy ion collisions obtain estimates for T_A using extensions of the HRGM that consider the nuclei as point-like particles [57] or assume the hard-core radius of all light (anti)nuclei to be equal to the hard-core radius of baryons R_b [58]. It is

of interest to go a step further and aim to describe nuclei in a more realistic way.

In our previous work [60] a more elaborate HRGM has been presented that is based on the concept of induced surface tension [36,37,38]. It uses an approximate expression for the hard-core radius of light (anti)nuclei denoted as bag model approximation (see below). This restriction was overcome recently in [62], where it was shown that the bag model approximation can safely be used for pion-dominated matter. However, the derivation of the equation of state (EoS) which extends the induced surface tension concept to the classical second virial coefficients of light (anti)nuclei as suggested in [40] is a heuristic one.

In the present work we develop a mathematically rigorous treatment of a mixture of hadrons and light (anti)nuclei with hard-core repulsion based on the induced surface tension concept [36,37,38]. In addition, with the help of this newly developed HRGM we analyze here not only the ALICE $\sqrt{s_{NN}} = 2.76$ TeV data on light (anti)nuclei [45,46,47], but also the STAR $\sqrt{s_{NN}} = 200$ GeV data [42,43,44]. [Our experience on achieving the accurate description of the hadronic data documented in Refs. \[25,26,27,28,29,30,31,33,34,37,38\] gives us a confidence that an essential improvement of the light nuclei data description will help the community to resolve the puzzles of the CFO of light nuclei.](#)

The work is organized as follows. In Sect. 2 the mathematically rigorous derivation of the induced surface tension EoS for the mixture of hadrons and nuclei with classical second virial coefficients is presented. Sect. 3 contains the results on two models of the CFO of light (anti)nuclei produced in the central A+A collisions on LHC and RHIC. Sect. 4 is devoted to the discussion of the obtained results and summarizes our conclusions.

2 Self-Consistent Treatment of Classical Excluded Volumes

In this section, we briefly show how to extend the method of self-consistent treatment of classical systems with multi-component hard-core interaction to the case of interaction of hadrons and light nuclei. It was introduced in [39] and successfully applied in [40] to mixtures of classical hard spheres and hard discs of different sizes.

There are three major reasons to consider the HRGM with multicomponent hard-core repulsion as the most realistic EoS of hadron matter at high temperatures and moderate particle number densities. First, a long time ago it was found that for temperatures below 170 MeV and moderate baryonic charge densities (below the nuclear saturation density) the mixture of stable hadrons whose interaction is described by the quantum second virial coefficients behaves almost like a mixture of ideal gases of particles in which both the stable hadrons and their resonances are included, but the latter should have the averaged vacuum values of masses [48]. As it was demonstrated in Ref. [48] and recently discussed in Ref. [49], the main physical reason for this kind of behavior is rooted in an

almost complete cancellation between the attractive and repulsive terms in the quantum second virial coefficients. Hence, the remaining deviation from the ideal gas (a weak repulsion) can be modeled by the classical hard-core repulsion.

Second, considering the HRGM as the EoS of hadronic matter one can be sure that its pressure will never exceed the one of the quark-gluon plasma. The latter may occur, if the hadronic phase is modelled as the mixture of ideal gases [38,51]. It is well-known that the number of spin-isospin degeneracies of all known hadrons and their resonances with the masses up to 2.6 GeV is so large that, if one ignores the hard-core repulsion between them, at temperatures above 180 MeV their pressure will be larger than the pressure of the quark-gluon plasma. An example of comparing the HRGM EoS with the lattice QCD results can be seen in Fig. 8 of Ref. [38].

Third, an additional and important reason to consider the HRGM as the hadronic matter EoS in the vicinity of CFO is a purely practical one: the hard-core repulsion is a contact interaction and, hence, the energy per particle of such an EoS coincides with the one of the ideal gas, even for the case of quantum statistics [52]. Consequently, during the evolution of the system after CFO to the kinetic freeze-out one will not face a hard mathematical problem [53,54] to somehow “transform“ the potential energy of interacting particles into their kinetic energy and into the masses of particles which appear due to resonance decays.

These are the main reasons which allow one to regard the HRGM as an extension of the statistical bootstrap model [55] supplemented by the hard-core repulsion, but for a truncated hadronic mass-volume spectrum, and which allow one to successfully apply it to the description of hadronic multiplicities measured in the central heavy ion collision experiments.

Although during last few years several valuable results were obtained with the help of HRGM [25,26,27,28,30,31,32,33,34,56], at the moment the hard-core radii are well established for the most abundant hadrons, i.e. for pions, for the lightest K^\pm -mesons, for nucleons and for the lightest (anti) Λ -hyperons. Nevertheless, the HRGM based on classical virial coefficients is very successful in describing the properties of a hadron gas at CFO temperatures above 50 MeV, hence it is natural to apply it to the description of multiplicities of atomic nuclei measured in A+A collision experiments instead of calculating their quantum virial coefficients.

However, even finding the classical excluded volumes of light (anti)nuclei consisting of A baryons is, in general, a highly nontrivial task, since there is no well-developed formalism to calculate the cluster integrals of the particles which are clusters themselves. Due to this reason the usual Mayer procedure to calculate such cluster integrals cannot be used in the general case. Furthermore, even the classical excluded volumes of light (anti)nuclei with hadrons are known the next nontrivial task is to rigorously derive the corresponding system of equations which can be used for the actual fitting of the data.

Nucleus	R_{rms} (fm)	classical distance $L(R_{\text{rms}})$	L (fm)
deuteron	2.1421 ± 0.0088	$2R_{\text{rms}}$	4.280
triton	1.7591 ± 0.0363	$\sqrt{3}R_{\text{rms}}$	3.047
^3He	1.9661 ± 0.0030	$\sqrt{3}R_{\text{rms}}$	3.405
^4He	1.6755 ± 0.0028	$4R_{\text{rms}}/\sqrt{6}$	2.739
$^3_{\Lambda}\text{H}$	4.9 (Ref. [65])	$\sim \sqrt{3}R_{\text{rms}}$	8.487

Table 1. The rms radii of light nuclei R_{rms} (2-nd column) taken from [64], except for the $^3_{\Lambda}\text{H}$ nuclei which is an estimate of Ref. [65]. The 3-rd column shows the relation between the typical distance among the constituents L and the rms radius R_{rms} of light nuclei, whereas the 4-th column provides the actual estimates for $L(R_{\text{rms}})$. See text for details.

Fortunately, the light nuclei of A baryons with $A \in [2; 4]$ are roomy clusters, i.e. their root mean square (rms) radii $R_{\text{rms}} = \sqrt{\langle r^2 \rangle}$ are rather large [63,64] as one can see from the second column of Table 1. This fact allows us to easily find out their classical second virial coefficient with the hadrons if the hard-core radii of all constituents of the considered nuclei are known. Assuming that the light nuclei of A baryons can be considered as the quasi-classical particles which slowly move around the common center-of-mass on the distance R_{rms} , one can estimate the typical distance between the constituents $L(R_{\text{rms}})$ in such nuclei. For the (anti)deuteron the typical distance between the (anti)nucleons is $L(R_{\text{rms}}) \simeq 2(R_{\text{rms}})$, while to estimate such a distance for triton, ^3He , $^3_{\Lambda}\text{H}$ and their antiparticles we suppose that they are the equilateral triangles. In this case, R_{rms} is the radius of the circle described around the equilateral triangle and, hence, the classical distance between the constituents inside such nuclei is $L(R_{\text{rms}}) \simeq \sqrt{3}R_{\text{rms}} \simeq 1.732R_{\text{rms}}$. Similarly, for the ^4He nucleus and its antiparticle, we assume that the nucleons form an equilateral tetrahedron with the radius of the sphere described around it being R_{rms} . Then the classical distance between the constituents of the ^4He nucleus is $L(R_{\text{rms}}) \simeq 4R_{\text{rms}}/\sqrt{6} \simeq 1.633R_{\text{rms}}$. These simple formulae and the actual estimates of $L(R_{\text{rms}})$ for different light nuclei are, respectively, given in the 3-rd and 4-th columns of Table 1.

Comparing the typical distances $L(R_{\text{rms}}^A)$ between the constituents of A baryons nuclei with the sum of largest hard-core diameter of hadrons 0.84 fm [36,37] and the hard-core diameter of baryons $2R_b = 0.73$ fm [36,37], one concludes that it is possible to freely translate the hadron with the hard-core radius R_h around each of the nucleus constituent, i.e. a baryon of hard-core radius $R_b = 0.365$ fm, without touching any other constituent of this nucleus [62]. Therefore, the classical second virial coefficient (excluded volume per particle) of a hadron and a nucleus of A baryons can be written as

$$b_{Ah} = b_{hA} = A \frac{2}{3} \pi (R_b + R_h)^3, \quad (1)$$

where R_b is the hard-core radius of baryons.

Similarly, we introduce the classical second virial coefficient (excluded volumes per particle) $b_{h_1 h_2}$ of hadrons of radii R_{h_1} and R_{h_2} as

$$b_{h_1 h_2} = b_{h_2 h_1} \equiv \frac{2}{3} \pi (R_{h_1} + R_{h_2})^3. \quad (2)$$

Now we consider a mixture of hadrons and light nuclei as Boltzmann particles with hard-core interaction. Neglecting for a moment the nucleus-nucleus interaction, i.e. assuming that $b_{A_1 A_2} = 0$, one can write the total excluded volume of such a mixture as

$$V_{\text{excl}}^{\text{tot}} = \sum_{k \in h_1, A_1} \sum_{l \in h_2, A_2} N_k b_{kl} N_l, \quad (3)$$

where N_k (N_l) is either the number of hadrons of sort h or the number of nuclei of A baryons. Note that in the sums in Eq. (3) the antiparticles are considered as the independent sorts of particles.

It is convenient to introduce the additional degeneracy of nuclei of A baryons g_{kA} and explicitly write the second virial coefficient (1) as

$$b_{kh_l} = g_{kA} \frac{2}{3} \pi (R_k + R_{h_l})^3 = g_{kA} \frac{2}{3} \pi \times \\ \times (R_k^3 + 3R_k^2 R_{h_l} + 3R_k R_{h_l}^2 + R_{h_l}^3), \quad (4)$$

$$\text{where } g_{kA} \equiv A \delta_{kA} + \delta_{kh}, \text{ and } g_{AA} R_A^n = A R_b^n, \quad (5)$$

where δ_{kA} and δ_{kh} are the Kronecker δ symbols.

Using the fact that the mean number of light nuclei $\langle N_A \rangle$ is very small compared to the mean number of all other hadrons $\sum_h \langle N_h \rangle$, i.e. $\langle N_A \rangle \ll \sum_h \langle N_h \rangle$, for light nuclei we can also write

$$A \langle N_A \rangle \ll \sum_h \langle N_h \rangle, \quad (6)$$

which allows us to approximate Eq. (3) as

$$V_{\text{excl}}^{\text{tot}} \simeq \frac{2}{3} \pi \sum_{k \in h_1, A_1} \sum_{l \in h_2, A_2} N_k g_{kA_1} \times \\ \times (R_k^3 + 3R_k^2 R_l + 3R_k R_l^2 + R_l^3) N_l g_{lA_2}, \quad (7)$$

where we substituted the binomial expression (4) for nucleus-hadron interaction and a similar binomial formula for the hadron-hadron interaction into Eq. (3). In addition in Eq. (7) the double summation is extended by adding the second degeneracy factor g_{lA_2} to account for the nucleus-nucleus interaction in a symmetric way which is convenient for further evaluation. Due to the inequality (6) which is valid for light nuclei the approximated Eq. (7) is rather accurate for A+A collisions.

Combining the first term in the brackets of Eq. (7) with the last term, and the second term with the third one, it is possible to identically rewrite the total excluded volume (7) in a shorter form

$$V_{\text{excl}}^{\text{tot}} \simeq \frac{4}{3} \pi \sum_{k \in h_1, A_1} \sum_{l \in h_2, A_2} N_k g_{kA_1} (R_k^3 + 3R_k^2 R_l) N_l g_{lA_2}, \quad (8)$$

which can be used to determine the mean excluded volume of the system per particle

$$\bar{V}_{excl} = V_{excl}^{tot} / \sum_{l \in h, A} N_l \simeq V_{excl}^{tot} / \sum_{l \in h, A} N_l g_{lA} \simeq \quad (9)$$

$$\simeq \sum_{k \in h_1, A_1} N_k g_{kA_1} V_k + \sum_{k \in h_1, A_1} N_k g_{kA_1} S_k \bar{R}, \quad (10)$$

where we introduced the eigen volume $V_k = \frac{4}{3}\pi R_k^3$ and eigen surface $S_k = 4\pi R_k^2$ of the particle of hard-core radius R_k and the mean hard-core radius \bar{R} defined as

$$\bar{R} = \sum_{k \in h, A} N_k g_{kA} R_k / \sum_{l \in h, A} N_l. \quad (11)$$

To obtain Eqs. (9)-(11) we, apparently, employed the inequality (6). In the thermodynamic limit Eqs. (10) and (11) enable us to self-consistently determine the EoS of the considered mixture within the VdW approximation.

To proceed further, we assume that for an infinite system one can replace all N_k values in (11) by their statistical mean values $\langle N_k \rangle$ and write

$$\bar{R} \rightarrow \sum_{k \in h, A} \langle N_k \rangle g_{kA} R_k / \sum_{l \in h, A} \langle N_l \rangle. \quad (12)$$

where $\langle N_l \rangle$ will be calculated self-consistently using the grand canonical ensemble (GCE) partition function. This means that using \bar{V}_{excl} (10) with \bar{R} defined by Eq. (12) one can calculate the GCE partition function regarding \bar{R} as a function of temperature T and chemical potentials $\{\mu_k\}$ and afterwards one can find \bar{R} from the calculated partition.

Denoting the chemical potential for the k -th sort of particles as μ_k , one can write the GCE partition function as

$$Z(T, \{\mu_k\}, V) \equiv \sum_{\{N_k\}} \left[\prod_{k \in h, A} \frac{[\phi_k e^{\frac{\mu_k}{T}} (V - \bar{V}_{excl})]^{N_k}}{N_k!} \right] \theta(V - \bar{V}_{excl}). \quad (13)$$

In Eq. (13) the thermal density ϕ_k of the k -th sort of particles contains the Breit-Wigner mass attenuation. In the Boltzmann approximation ϕ_k can be written as

$$\phi_k = g_k \gamma_S^{|s_k|} \int_{M_k^{Th}}^{\infty} \frac{dm}{N_k (M_k^{Th})} \frac{\Gamma_k}{(m - m_k)^2 + \Gamma_k^2/4} \times \int \frac{d^3p}{(2\pi\hbar)^3} \exp\left[-\frac{\sqrt{p^2+m^2}}{T}\right], \quad (14)$$

where g_k denotes the degeneracy factor of the k -th sort of particle, γ_S is its strangeness suppression factor [66], $|s_k|$ is the number of valence strange quarks and antiquarks in this sort of particle, while the factor

$$N_k(M_k^{Th}) \equiv \int_{M_k^{Th}}^{\infty} \frac{dm \Gamma_k}{(m - m_k)^2 + \Gamma_k^2/4} \quad (15)$$

denotes a normalization constant, in which M_k^{Th} denotes the decay threshold mass of the k -th hadronic resonance, while Γ_k denotes its width. Clearly, for the stable hadrons and light nuclei the width Γ_k should be set to zero, which leads to the familiar expression for the thermal density

$$\phi_k = g_k \gamma_S^{|s_k|} \int \frac{d^3p^3}{(2\pi\hbar)^3} \exp\left[-\frac{\sqrt{p^2+m_k^2}}{T}\right]. \quad (16)$$

We would like to stress that the Breit-Wigner ansatz for the mass attenuation is an approximation which is usually valid for relatively narrow resonances only. However, the expression for thermal density of unstable particles (14) in the spirit of a Beth-Uhlenbeck EoS [67] is valid for more general mass distributions which may replace this ansatz. For some dynamical models of hadron structure such as the NJL model, one could separate the resonant part of the interaction which would correspond to an unstable hadronic state and can be approximated by a Breit-Wigner ansatz and the residual, repulsive interaction [68, 69, 70]. This is fortunate if the approach shall be combined with an excluded volume model for the short-range repulsion, in order to avoid a possible double counting. The generalized Beth-Uhlenbeck EoS can be rigorously derived for a mixture of hadron resonances [72, 73] from a cluster decomposition of the Phi-functional approach [74], if the generalized Phi-functional belongs to the class of cluster two-loop diagrams [75, 11].

Note that the Heaviside step function θ in Eq. (13) is very important, since it ensures the absence of negative values of the available volume ($V - \bar{V}_{excl}$) and provides the finite number of all particles for finite volume of the system V . However, due to its presence, the evaluation of the GCE partition function (13) is hard. To overcome this difficulty one should make the Laplace transformation with respect to V to the isobaric partition (for an appropriate review see [76]) which is defined as

$$\mathcal{Z}(T, \{\mu_k\}, \lambda) \equiv \int_0^{\infty} dV e^{-\lambda V} Z(T, \{\mu_k\}, V). \quad (17)$$

Below we show that the isobaric partition $\mathcal{Z}(T, \{\mu_k\}, \lambda)$ can be found exactly by changing the integration variable $dV \rightarrow d(V - \bar{V}_{excl})$. However, first of all it is necessary to define the quantities $\langle N_k \rangle$ in the GCE variables. In terms of the partial μ_k -derivative of the partition (13), one can define $\langle N_k \rangle$ as follows

$$\langle N_k \rangle \equiv T \frac{\partial}{\partial \mu_k} \ln[Z(T, \{\mu_l\}, V)]. \quad (18)$$

In terms of definition (18) Eq. (12) for \bar{R} can be cast as

$$\bar{R} = \frac{\sum_{k \in h, A} g_{kA} R_k \frac{\partial}{\partial \mu_k} \ln[Z(T, \{\mu_l\}, V)]}{\sum_{k \in h, A} \frac{\partial}{\partial \mu_k} \ln[Z(T, \{\mu_l\}, V)]}. \quad (19)$$

Changing the variable $dV \rightarrow d(V - \bar{V}_{excl})$ in Eq. (17), one finds

$$\mathcal{Z}(T, \{\mu_k\}, \lambda) = \int_0^\infty dV' e^{-\lambda V'} \times \sum_{\{N_k\}} \prod_{k \in h, A} \frac{1}{N_k!} \left[\phi_k e^{\frac{\mu_k}{T}} V' \right]^{N_k} e^{-\lambda \bar{V}_{excl} \theta(V')}. \quad (20)$$

Substituting into Eq. (20) the expression (10) for \bar{V}_{excl} , one gets

$$\begin{aligned} \mathcal{Z}(T, \{\mu_k\}, \lambda) &= \\ &= \int_0^\infty dV' e^{-\lambda V'} \sum_{\{N_k\}} \prod_{k \in h, A} \frac{\left[\phi_k e^{\frac{\mu_k}{T} - \lambda g_{kA} (V_k + \bar{R} S_k)} V' \right]^{N_k}}{N_k!} = \\ &= \int_0^\infty dV' \exp \left[V' \left[\sum_{k \in h, A} \phi_k e^{\frac{\mu_k}{T} - \lambda g_{kA} (V_k + \bar{R} S_k)} - \lambda \right] \right]. \quad (21) \end{aligned}$$

Integration with respect to variable dV' in Eq. (21) can be done easily resulting in

$$\mathcal{Z}(T, \{\mu_k\}, \lambda) = \frac{1}{\lambda - \mathcal{F}(\lambda, T, \{\mu_k\})}, \quad (22)$$

where the function $\mathcal{F}(\lambda, T, \{\mu_k\})$ which defines the system pressure in the thermodynamic limit is given by

$$\mathcal{F}(\lambda, T, \{\mu_k\}) = \sum_{k \in h, A} \phi_k \exp \left[\frac{\mu_k}{T} - \lambda g_{kA} [V_k + S_k \bar{R}] \right]. \quad (23)$$

The GCE partition function (13) can be found now by the inverse Laplace transform

$$\begin{aligned} Z(T, \{\mu_k\}, V) &= \frac{1}{2\pi i} \int_{\chi-i\infty}^{\chi+i\infty} d\lambda e^{\lambda V} \mathcal{Z}(T, \{\mu_k\}, \lambda) = \\ &= \frac{e^{\lambda^* V}}{1 - \frac{\partial \mathcal{F}}{\partial \lambda}(\lambda, T, \{\mu_k\})} \Big|_{\lambda=\lambda^*}. \quad (24) \end{aligned}$$

As usual, in Eq. (24) the integration contour in the complex λ -plane is chosen to the right-hand side of the rightmost singularity λ^* , i.e. $\chi > \lambda^*$ (more details can be found in Ref. [76]). Since the number of hadronic states and light nuclei used in the HRGM is finite [36, 37], then the sum in Eq. (24) contains the finite number of terms and, hence, as shown in Ref. [76], the isobaric partition (24) has only the simple pole at $\lambda = \lambda^*$. The latter is a solution of the equation

$$\lambda^* = \mathcal{F}(\lambda^*, T, \{\mu_k\}). \quad (25)$$

In the thermodynamic limit $V \rightarrow \infty$ from Eq. (24) one finds the system pressure as $p \equiv T\lambda^*$, since in this limit the GCE partition behaves as $Z(T, \{\mu_k\}, V \rightarrow \infty) \sim \exp(pV/T)$ [77].

Using Eq. (25) one can write for the pressure

$$p = T \sum_{k \in h, A} \phi_k \exp \left[\frac{\mu_k - p g_{kA} [V_k + \bar{R} S_k]}{T} \right], \quad (26)$$

which should be supplemented by the equation for the mean hard-core radius \bar{R} . Using Eq. (24) one can rewrite Eq. (19) as follows

$$\bar{R} = \frac{\sum_{k \in h, A} g_{kA} R_k \frac{\partial}{\partial \mu_k} [\lambda^* V - \ln(1 - \frac{\partial \mathcal{F}}{\partial \lambda^*})]}{\sum_{k \in h, A} \frac{\partial}{\partial \mu_k} [\lambda^* V - \ln(1 - \frac{\partial \mathcal{F}}{\partial \lambda^*})]}. \quad (27)$$

In the thermodynamic limit $V \rightarrow \infty$ the terms $\ln(1 - \frac{\partial \mathcal{F}}{\partial \lambda^*})$ in Eq. (27) are small compared to the term $\lambda^* V$. Hence, finding the partial derivatives $\frac{\partial \lambda^*}{\partial \mu_k}$ from Eq. (25), in the limit $V \rightarrow \infty$ one can rewrite Eq. (27) as

$$\bar{R} = \frac{\sum_{k \in h, A} g_{kA} R_k \phi_k \exp \left[\frac{\mu_k - p g_{kA} [V_k + S_k \bar{R}]}{T} \right]}{\sum_{k \in h, A} \phi_k \exp \left[\frac{\mu_k - p g_{kA} [V_k + S_k \bar{R}]}{T} \right]}. \quad (28)$$

With the help of equation (26) for pressure it is convenient to cast the last result in terms of the induced surface tension (IST) coefficient [36]

$$\begin{aligned} \Sigma &\equiv p\bar{R} = \\ &= T \sum_{k \in h, A} g_{kA} R_k \phi_k \exp \left[\frac{\mu_k - p g_{kA} V_k - \Sigma g_{kA} S_k}{T} \right]. \quad (29) \end{aligned}$$

Rewriting equation for pressure similarly, one gets

$$\begin{aligned} p &= \sum_{k \in h, A} p_k = \\ &= T \sum_{k \in h, A} \phi_k \exp \left[\frac{\mu_k - p g_{kA} V_k - \Sigma g_{kA} S_k}{T} \right], \quad (30) \end{aligned}$$

where the partial pressures $\{p_k\}$ of each sort of particles are introduced for convenience.

The system of Eqs. (29) and (30) for the IST coefficient Σ and pressure p , respectively, defines the EoS of the mixture of hadrons and light nuclei within the VdW approximation. Note that in contrast to the heuristic derivation of such a system suggested in [62] the present derivation of the system (29) and (30) is rigorous and well-controlled. The applicability range of the VdW approximation is, unfortunately, rather narrow and, therefore, its usage at the packing fractions $\eta = \sum_{k \in h, A} g_{kA} V_k \rho_k$ (here $\rho_k = \frac{\partial p}{\partial \mu_k}$ is the particle number density) above 0.12-0.15 may lead to problems with causality [37, 38, 78] (a typical example of acausal HRGM can be found in Ref. [79], see also its critique in Refs. [37, 38]).

Fortunately, the applicability range of the system (29) and (30) can be extended to higher values of packing fractions in a simple way. The main idea of the IST approach

[36,37,38,39,40] is that at high pressures the mean radius \bar{R} in Eqs. (26), (8) and (29) should be suppressed stronger than it is provided by the VdW approximation. Then for increasing pressure the mean radius \bar{R} should gradually vanish leading to a reduction of the effective excluded volume of particle of k -th sort which is defined as

$$V_k^{eff} = g_{kA} \frac{(V_k p + S_k \Sigma)}{p} \rightarrow \begin{cases} g_{kA}(V_k + S_k \bar{R}), & \text{for } \frac{\max[V_h]p}{T} \ll 1, \\ g_{kA}V_k, & \text{for } \frac{\max[V_h]p}{T} \gg 1. \end{cases} \quad (31)$$

In other words, a gradual vanishing of the mean hard-core radius \bar{R} should provide a slow transformation of the VdW (excluded volume) approximation, which is valid at low packing fractions $\eta \leq 0.1$, into the eigen volume approximation, which is valid at high packing fractions $\eta > 0.5$ [77,80]. As suggested in Ref. [36] and verified in Refs. [37,38,39,40] such an additional suppression of \bar{R} can be obtained by replacing the term ΣS_k on the right hand side of Eq. (29) as

$$\Sigma S_k \rightarrow \Sigma S_k \alpha_k, \quad \text{where } \alpha_k > 1, \quad (32)$$

where the auxiliary parameters α_k should be chosen in such a way that they describe the higher virial coefficients. Under this generalization Eq. (29) becomes

$$\begin{aligned} \Sigma &= \sum_{k \in h,A} \Sigma_k = \\ &= T \sum_{k \in h,A} g_{kA} R_k \phi_k \exp \left[\frac{\mu_k - g_{kA}(pV_k + \alpha_k \Sigma S_k)}{T} \right], \end{aligned} \quad (33)$$

where Σ_k denotes the surface tension coefficient of k -th sort of particles. In this way one can account not only for the second virial coefficients, but also for the higher order virial coefficients as demonstrated for systems with single-component hard-core repulsion in Refs. [37,38,39] and for two-component mixtures studied recently in [40].

The reason to chose all the parameters α_k as $\alpha_k > 1$ becomes apparent after analyzing the effective excluded volume (31). Indeed, substituting Eq. (33) into Eq. (31) one finds for hadrons

$$V_k^{eff} \equiv V_k + S_k \frac{\sum_{l \in h,A} p_l R_l e^{-(\alpha_l - 1) S_l \Sigma / T}}{\sum_{n \in h,A} p_n}. \quad (34)$$

This equation shows that in the limit of low packing fractions, i.e. for $\Sigma \max[S_h]/T \ll 1$, each exponential in Eq. (34) is $\exp \left[-\frac{(\alpha_l - 1) S_l \Sigma}{T} \right] \simeq 1$ and, hence, one recovers the upper Eq. (31). However, it is easy to show that for high packing fractions an opposite inequality $\frac{\Sigma S_k}{T} \gg 1$ is valid for any $S_k > 0$. In this case the condition $\alpha_k > 1$ provides the vanishing of the mean radius $\bar{R} \equiv \frac{\Sigma}{p}$ and, hence, in this limit the effective excluded volume of each particle

approaches its eigen volume, $V_k^{eff} \rightarrow V_k$. Thus, at high packing fractions Eq. (34) leads to the lower Eq. (31).

The system (30), (33) is a generalization of the IST EoS derived in Ref. [40] for the classical hard spheres onto the multicomponent mixture of hard spheres (hadrons) and roomy classical clusters which are the light nuclei of A baryons. As one can see from the derivation above such a generalization is not straightforward and contains some nontrivial steps. In particular, the inequality (6) played a crucial role in simplifying our derivation of the mean excluded volume per particle. Furthermore, the fact that the thermal density (14) of considered particles may, in principle, include the finite width opens an entirely new possibility to apply the present approach to the treatment of other roomy exotic clusters which have even larger width, than the hypertriton ${}^3_A\text{H}$ like, e.g., ${}^4\text{Li}$ and ${}^4\text{H}$ [6,41].

In fact, the system (30), (33) can be generalized further in the spirit of Refs. [39,40] in order to extend it to very high packing fractions $\eta \simeq 0.45 - 0.5$ by introducing into treatment the induced curvature tension.

In Refs. [37,38] it is shown that even with a single parameter $\alpha_k = \text{const} = \alpha = 1.245$ Eqs. (30), (33) for the classical hard spheres allows one to go beyond the VdW approximation, whereas in Ref. [40] one can find several examples on how two auxiliary parameters enables us to go far beyond the VdW approximation for two component classical systems. However, an extension of the system (30), (33) onto the quantum mechanical treatment of light (anti)nuclei in the spirit of Ref. [39] still remains a challenge for theoreticians.

3 Analysis of light nuclei multiplicities measured in A+A collisions

The system (30), (33) is the IST EoS with classical excluded volumes of (light) nuclei and, hence, hereafter it is called IST EoS in order to distinguish it from another treatment of hard-core repulsion developed in [60,62]. Although an approach of Refs. [60,62] is approximative, nevertheless, we consider it as a complementary one to the IST model. It is based on the idea to introduce the equivalent hard-core radius R_{Ah}^{eq} of a pair Ah by equating the excluded volume $\frac{2}{3}\pi(R_{Ah}^{eq})^3$ with the equivalent hard-core radius R_{Ah}^{eq} to the actual excluded volume of such a pair b_{Ah} given by Eq. (1). Then we get the equivalent hard-core radius as [62]

$$R_{Ah}^{eq} = A^{\frac{1}{3}}(R_b + R_h). \quad (35)$$

From the expression for R_{Ah}^{eq} one can determine the effective hard-core radius of a nucleus in a hadronic medium dominated by pions

$$R_A \simeq R_{A\pi}^{eq} - R_\pi \simeq A^{\frac{1}{3}}R_b + (A^{\frac{1}{3}} - 1)R_\pi \simeq A^{\frac{1}{3}}R_b. \quad (36)$$

It is necessary to stress that this approximation is well justified for the A+A of high energies by the fact that pions are the most abundant particles. In particular, this is the

case for the LHC and the highest RHIC collision energies. The term $(A^{\frac{1}{3}} - 1)R_\pi$ in Eq. (36) is a small correction to the effective hard-core radius of nuclei $R_A \simeq A^{\frac{1}{3}}R_b$, since the hard-core radius of pions $R_\pi \simeq 0.15$ fm [36,37] is essentially smaller than the one of baryons $R_b = 0.365$ fm and the hard-core radii of kaons $R_K = 0.395$ fm and other mesons $R_m = 0.42$ fm. Therefore, for low values of baryonic chemical potential (roughly for $\mu_B < T$) the pions are the least suppressed by the hard-core repulsion and, consequently, for any $A \leq 4$ the correction $(A^{\frac{1}{3}} - 1)R_\pi \leq 0.088$ fm in Eq. (36) can be safely neglected for the pion-dominated hadronic medium.

The hard-core radius of light (anti)nuclei (36) is similar to the expression of the Bag Model radius (BMR) [81] of large bags of quark-gluon plasma and, hence, hereafter this model is called the BMR EoS. Despite the fact that it is an approximative approach, it is, however, simpler because with the help of the hard-core radius (36) the IST EoS allows one to treat the nuclei and hadrons exactly on the same footing. Moreover, *a simultaneous use of IST and BMR approaches allows us to introduce a new strategy to locate the CFO of light (anti)nuclei*. Since in the pion-dominated hadronic medium the BMR approach should give the same results as the IST, we have to search for the region of parameters at which both approaches provide a similar quality of the data description.

For the BMR approach the system (30), (33) should be slightly modified. Then formally considering the light (anti)nuclei as the primed sorts of hadrons h'_A (with $A = 2, 3, 4$), we can write

$$p = \sum_{k \in h, h'_A} p_k = T \sum_{k \in h, h'_A} \phi_k \exp \left[\frac{\mu_k - pV_k - \Sigma S_k}{T} \right], \quad (37)$$

$$\begin{aligned} \Sigma &= \sum_{k \in h, h'_A} \Sigma_k = \\ &= T \sum_{k \in h, h'_A} R_k \phi_k \exp \left[\frac{\mu_k - pV_k - \alpha_k \Sigma S_k}{T} \right], \end{aligned} \quad (38)$$

where the hard-core radii of primed hadrons are given by Eq. (36).

The partial values p_k and Σ_k entering the system (30), (33) (or (37), (38)) allow one to write the particle number density of k -th sort of particle in a simple way

$$\rho_k \equiv \frac{\partial p}{\partial \mu_k} = \frac{1}{T} \cdot \frac{p_k a_{22} - \Sigma_k a_{12}}{a_{11} a_{22} - a_{12} a_{21}}. \quad (39)$$

For the system (37), (38) the coefficients a_{kl} are given by [37]

$$a_{11} = 1 + \frac{4}{3} \pi \sum_{k \in h, h'_A} R_k^3 \frac{p_k}{T}, \quad a_{12} = 4\pi \sum_{k \in h, h'_A} R_k^2 \frac{p_k}{T}, \quad (40)$$

$$a_{21} = \frac{4}{3} \pi \sum_{k \in h, h'_A} R_k^3 \frac{\Sigma_k}{T}, \quad a_{22} = 1 + 4\pi \sum_{k \in h, h'_A} R_k^2 \alpha_k \frac{\Sigma_k}{T}, \quad (41)$$

while in order to calculate the particle number densities for the system (30), (33) in Eqs. (40) and (41) one has to

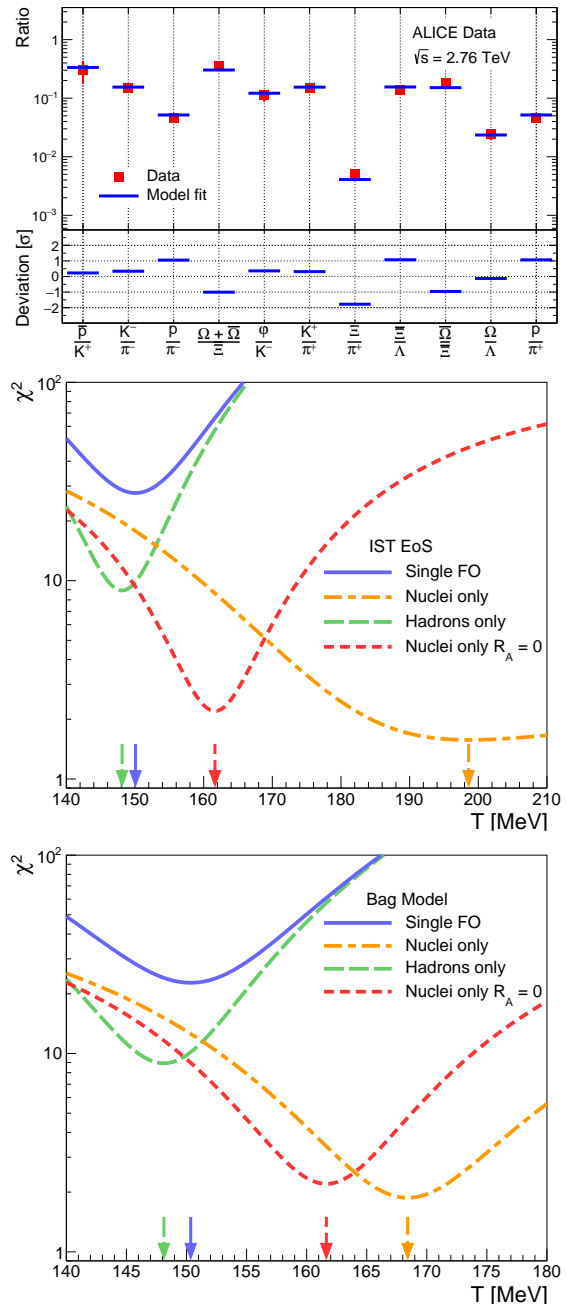


Fig. 1. Upper panel: Ratios of hadronic yields measured at $\sqrt{s_{NN}} = 2.76$ TeV (symbols) vs. the results of IST EoS (30), (33) (bars, for more details see the text). The CFO temperatures $T_A = T_h = 150.1 \pm 1.9$ MeV are for the single CFO IST EoS. Insertion shows the deviation of theory from data in the units of experimental error. **Middle panel:** Temperature dependence of χ_{tot}^2 , χ_h^2 and χ_A^2 for the IST EoS. **Lower panel:** Same as in the middle panel, but for the BMR EoS.

make the following replacements

$$R_{h'_A}^2 \rightarrow AR_b^2, \quad R_{h'_A}^3 \rightarrow AR_b^3, \quad (42)$$

for the powers of hard-core radius of A baryons nucleus. After finding all partial values $\{p_k\}$ and $\{\Sigma_k\}$, from the

expressions (39)-(41) one can determine the thermal yield $N_k^{th} = V\rho_k$ of the k -th sort of particles. For hadrons, however, one has also to add the contribution coming from the decays of resonances. For the known branching ratios $Br_{l \rightarrow k}$ of hadronic decays $l \rightarrow k$ one can write the total yield of k -th sort of hadrons as follows

$$N_k^{tot} = V \left(\rho_k + \sum_{l \neq k} \rho_l Br_{l \rightarrow k} \right), \quad (43)$$

where V is the CFO volume. Since all details of the fitting process are well presented in the original works [37,38], here we discuss the most important issues only.

To analyze the ALICE data [45,46,47] we use the setup of Ref. [37], while for the analysis of the STAR data that of Ref. [38]. The main difference in fitting the hadrons and the A -baryon nuclei is that for hadrons we use the ratios

$$\mathcal{R}_{kl}^{theo} = \frac{\rho_k + \sum_{n \neq k} \rho_n Br_{n \rightarrow k}}{\rho_l + \sum_{n \neq k} \rho_n Br_{n \rightarrow l}}, \quad (44)$$

of yields of hadrons of sorts k and l . On contrary for the A baryon nuclei we employ the yields. Hence the total $\chi_{tot}^2(V)$ used in the present work is

$$\begin{aligned} \chi_{tot}^2(V) &= \chi_h^2 + \chi_A^2(V) = \\ &= \sum_{k \neq l \in h} \left[\frac{\mathcal{R}_{kl}^{theo} - \mathcal{R}_{kl}^{exp}}{\delta \mathcal{R}_{kl}^{exp}} \right]^2 + \sum_A \left[\frac{\rho_A(T)V - N_A^{exp}}{\delta N_A^{exp}} \right]^2. \end{aligned} \quad (45)$$

Here χ_h^2 and χ_A^2 denote, respectively, the mean deviation squared for hadrons and (anti)nuclei. Note that $\chi_{tot}^2(V)$ is a function of the CFO volume V . This is an important difference from our previous analyses of [25,26,27,29,37,38], which, as we will show below, allows us to elucidate the new details on the CFO of light (anti)nuclei. Since now on we also consider a single value $\alpha_k = 1.25$ [37,38].

First, we apply the single CFO model to the ALICE data description. The hadronic data were taken from Refs. [82,83,84,85]. In the HRGM it is traditionally assumed that the CFO occurs for all particles simultaneously. The principal results are given in Table 2 and Figs. 1 and 2. To get these results we calculated the χ_{tot}^2 using 2 fitting parameters, i.e. the CFO temperature and the CFO volume of nuclei $V = V_A$, for 11 hadronic ratios and 8 yields of light (anti)nuclei. All the chemical potentials are set to zero, while $\gamma_s = 1$ is fixed according to Refs.[37,38]. The hard-core radii of hadrons are taken from our previous works [37,38] (are listed above). These values provide an excellent description of hadron yield ratios from AGS to LHC energies.

As one can see from Fig. 1 and from Table 2 the quality of ALICE data description obtained for the single CFO scenario is similar for the IST and BMR EoS. Moreover, the corresponding CFO temperatures are very similar, since the χ_{tot}^2 is completely defined by the hadronic contribution to χ_{tot}^2 . Although the obtained overall description is satisfactory with $\chi_{tot}^2/dof|_{IST} \simeq 1.627$ and $\chi_{tot}^2/dof|_{BMR} \simeq 1.336$, there are two surprising features in this scenario. First, $\chi_{tot}^2/dof|_{IST}$ found by the advanced

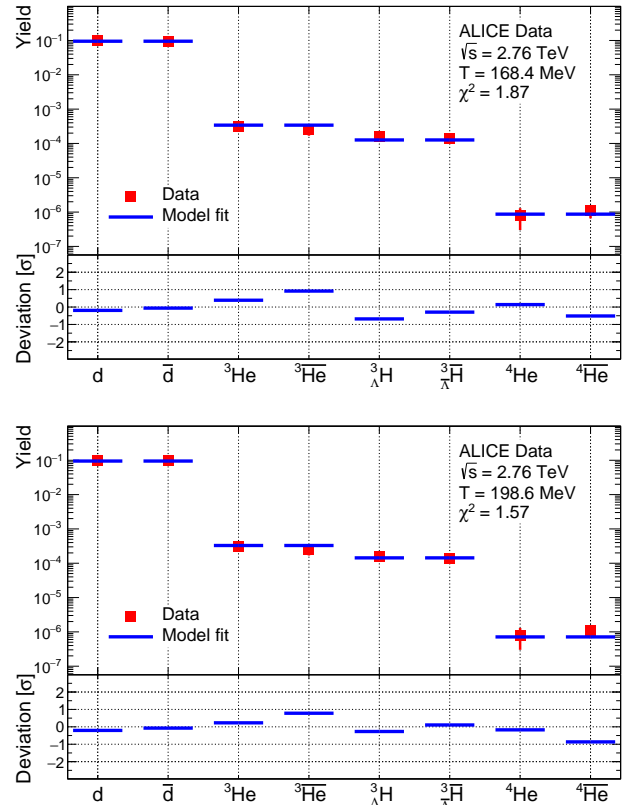


Fig. 2. The yields of nuclear clusters measured at $\sqrt{s_{NN}} = 2.76$ TeV vs. theoretical description in the scenario of separate CFO of light (anti)nuclei. **Upper panel:** The min $\chi_A^2(V)$ corresponds to the BMR EoS (third row in Table 2). **Lower panel:** Same as in the upper panel, but for the IST EoS (fourth row in Table 2).

model is somewhat larger than $\chi_{tot}^2/dof|_{BMR}$. Second, the CFO volumes of light (anti)nuclei are essentially larger than the CFO volume $V_h = \frac{N_{\pi^+}^{exp}}{\rho_{\pi^+} + \sum_{l \neq k} \rho_l Br_{l \rightarrow \pi^+}} \simeq 8165 \pm 600$ fm³ of hadrons found from the experimental multiplicity of positive pions $N_{\pi^+}^{exp}$. This is best seen, when applying the new strategy to determine the common CFO volume for nuclei which is found to be $V_A \in [11100; 13260]$ fm³. Comparing V_A with V_h one finds that min $V_A \simeq 11100$ fm³ is sizably larger than max $V_h \simeq 8765$ fm³. This means that at the same CFO temperature the emission volume of hadrons and nuclei are rather different, i.e. the nuclei are freezing out in a much larger volume which means that there is no common hyper-surface of CFO. In our opinion, both of these features evidence for the internal inconsistency of the single CFO scenario at ALICE energy of collisions. Therefore, following the original idea of Ref. [60], we verify the hypothesis of separate CFO of light (anti)nuclei.

From Fig. 1 one can see that at high CFO temperatures the quantity $\chi_A^2(V_A(T_A))$ has a deep minimum not only for the IST and BMR EoS, but even for the vanishing size of nuclei. In other words, the existence of a minimum of χ_A^2 at high temperatures is a generic feature of the

Description	T_h , MeV	T_A , MeV	V_A , fm ³	χ^2/dof
Single CFO, BMR	150.35 ± 1.91	150.35 ± 1.91	11241 ± 2016	1.336
Single CFO, IST	150.06 ± 1.94	150.06 ± 1.94	13357 ± 2277	1.627
Separate CFO, BMR	148.12 ± 2.03	168.41 ± 5.60	2997 ± 1164	0.675
Separate CFO, IST	148.12 ± 2.03	198.59 ± 30.47	1544 ± 1027	0.656

Table 2. The results obtained by the advanced HRGM for the fit of ALICE data measured at $\sqrt{s} = 2.76$ TeV. The CFO temperature of hadrons is T_h , the CFO temperature of light (anti)nuclei is T_A , while their CFO volume is V_A . The last column gives the fit quality.

advanced versions of HRGM. In the scenario of separate CFO of nuclei, there are three fitting parameters, namely the CFO temperatures of hadrons T_h and nuclei T_A , and the CFO volume of nuclei V_A . As one can see from Table 2 and from Figs. 1 and 2 one can see that the hypothesis of separate CFO of nuclei provides an excellent fit with $\chi_{tot}^2/dof|_{IST} \simeq 0.656$ and $\chi_{tot}^2/dof|_{BMR} \simeq 0.675$. Thus, compared to the single CFO scenario the value of χ_{tot}^2/dof in this case decreased by 50%.

However, the minimum of $\chi_A^2|_{IST}$ is located at essentially larger CFO temperature than the one found for the minimum of $\chi_A^2|_{BMR}$. Moreover, the found T_A for IST EoS is so large, that one can doubt the existence of hadrons and nuclei at this CFO temperature. Fortunately, with the help of the new strategy introduced in the preceding section one can resolve this problem easily. Indeed, similar results for the description of light (anti)nuclei by the IST and BMR EoS can be achieved in the vicinity of the common CFO temperature T_A^{com} defined by the equality

$$\chi_A^2(V(T_A^{com}))|_{IST} = \chi_A^2(V(T_A^{com}))|_{BMR} \Rightarrow \quad (46)$$

$$\Rightarrow T_A^{com} = 175.1_{-3.9}^{+2.3} \text{ MeV}, \quad (47)$$

where the common CFO temperature still corresponds to a very accurate description of the ALICE data for light (anti)nuclei $\chi_A^2(V(T_A^{com}))|_{IST} \simeq 3.2$ and $V_A^{com} = V_A(T_A^{com}) \simeq 2660_{-1160}^{+1010} \text{ fm}^3$. The upper and lower deviations from $T_A^{com} = 175.1$ MeV in Eq. (47) were found numerically by increasing the value of $\chi_A^2(V(T_A^{com}))|_{IST} \simeq 3.2$ on 1σ . Note that for $T_A^{com} = 175.1$ MeV the total value of $\chi_{tot}^2/dof = 12.123/16 \simeq 0.758$ is rather small, i.e. it still corresponds to a highly accurate description of the ALICE data. Furthermore, the found range of T_A^{com} is consistent with the values of CFO temperature found for the RHIC collision energy [37, 57, 56, 86] and it is a few MeV above the upper estimate for the cross-over temperature $T_{co} \simeq 147 - 170$ MeV predicted by the lattice formulation of QCD at vanishing value of the baryonic chemical potential [87, 88]. Therefore, we are confident that the HRGM is applicable at these values of the common CFO temperature.

It is necessary to mention that the above numbers differ slightly from our preliminary results of a similar analysis reported in Ref. [62]. The main difference is that in the present work we use the non-vanishing width for all hadronic resonances, while in Ref. [62] the solutions of systems (29), (30) and (37), (38) were found for zero width

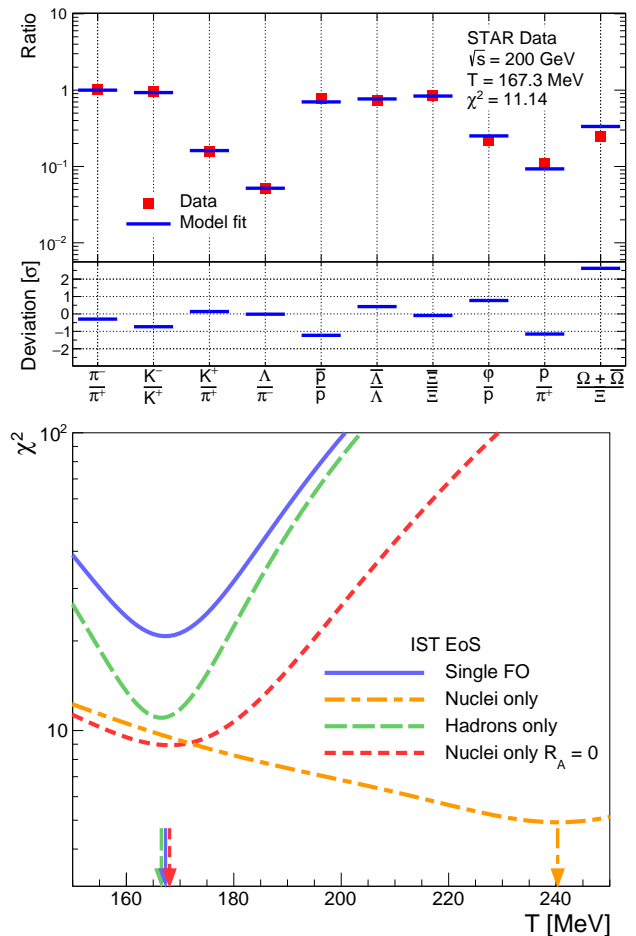


Fig. 3. **Upper panel:** Ratios of hadronic yields measured at $\sqrt{s_{NN}} = 200$ GeV (symbols) vs. the results of IST EoS (bars) (30), (33) (for more details see the text). The CFO temperatures $T_A = T_h = 167.28 \pm 3.93$ MeV are given for the single CFO IST EoS. Insertion shows the deviation of theory from data in the units of experimental error. **Lower panel:** Temperature dependence of χ_{tot}^2 , χ_h^2 and χ_A^2 for the IST EoS.

of all hadronic resonances in order to fasten the fit process. However, the value of $T_A^{com} = 175.1$ MeV found here and the result $T_A^{com} = 174.6$ MeV found in [62] are practically the same, whereas its uncertainty determined here is a couple of MeV larger than in Ref. [62].

The results of a similar analysis of the STAR data measured at $\sqrt{s} = 200$ GeV are presented in Table 3 and

Figs. 3 and 4. The STAR data consist of 10 hadronic ratios that are taken from Refs. [90,91,92] and are shown in the upper panel of Fig. 3, yields of (anti)deuterons [44], and 5 light (anti)nuclei yield ratios [42,43]. For the single CFO scenario, we have 3 fitting parameters, i.e. CFO temperature $T_h = T_A$, CFO baryonic chemical potential $\mu_B^A = \mu_B^h$ and the CFO volume of nuclei V_A . The strange chemical potential and the one of third projection of isospin are set to zero for simplicity, while $\gamma_s = 1$ according to Ref. [38].

The results obtained for the hadronic ratios are depicted in the upper panel of Fig. 3, while the CFO temperature scan of $\chi_{tot}^2(V(T_A = T_h))|_{IST}$ is shown in the lower panel of this figure. As one can see from Fig. 3 all hadronic ratios, except the ratio $\frac{\Omega+\bar{\Omega}}{\Xi}$, are well reproduced by the IST EoS. From Table 3 one can see that the CFO temperature T_h , the CFO baryonic chemical potential μ_B^h and χ_{tot}^2/dof obtained for the IST and BMR EoS are practically the same. But the most striking result is that for the single CFO scenario, the value of common CFO volume $V_A^{com} = 1898.5 \pm 157.5 \text{ fm}^3$ (see Table 3) is only 30 percent smaller compared to the corresponding value $V_A^{com} \simeq 2660_{-1160}^{+1010} \text{ fm}^3$ found above for the ALICE energy. *We believe this is a remarkable finding, since the collision energy of the ALICE data is about 14 times larger than the one of the STAR data.* At the same time for this scenario, the CFO volume of hadrons $V_h = 2808 \pm 253 \text{ fm}^3$ found via the density of positive pions is slightly larger.

For the scenario of separate CFO of light (anti)nuclei, the CFO temperature of nuclei is substantially higher than the one of hadrons as one can see from Table 3. Although the higher value of T_A provides a better description of the light (anti)nuclei yields as it is seen from Fig. 4, the value of $\chi_{tot}^2(V(T_A^{com}))/dof|_{IST} = \chi_{tot}^2(V(T_A^{com}))/dof|_{BMR} \simeq 1.61$ with $T_A^{com} \simeq 180 \pm 11.25 \text{ MeV}$ is about 10 percent larger than for the scenario of a single CFO. The reason is that for the scenario of separate CFO there are two additional parameters, namely the temperature of nuclei T_A and their baryonic chemical potential μ_B^A were fitted in this case. As a result, the number of degrees of freedom in this case is $17 - 5 = 12$. Therefore, in contrast to the ALICE data, the STAR data do not demonstrate any preference for the separate CFO of light (anti)nuclei. Furthermore, in our opinion, there is no reason to expect that CFO of light (anti)nuclei can occur at the CFO temperatures above 175-180 MeV, since the hadronic description at those CFO temperatures is rather problematic according to the contemporary lattice version of QCD [87, 88]. The recent lattice QCD result for the continuum-extrapolated chiral susceptibility at vanishing values of baryonic chemical potential define with high accuracy the pseudo-critical transition temperature $T_{pc} = 156.5 \pm 1.5 \text{ MeV}$ [89] from its peak position. However, it also demonstrated that this peak has a full-width at half maximum of about 40 MeV. Therefore we conclude that the STAR data which favor the single CFO scenario with $T_A^{com}|_{STAR} \simeq 167.22 \text{ MeV}$ and $V(T_A^{com})|_{STAR} \simeq 1898.5 \text{ fm}^3$ (see Table 3) is not in contradiction with the lattice QCD result of Ref. [89].

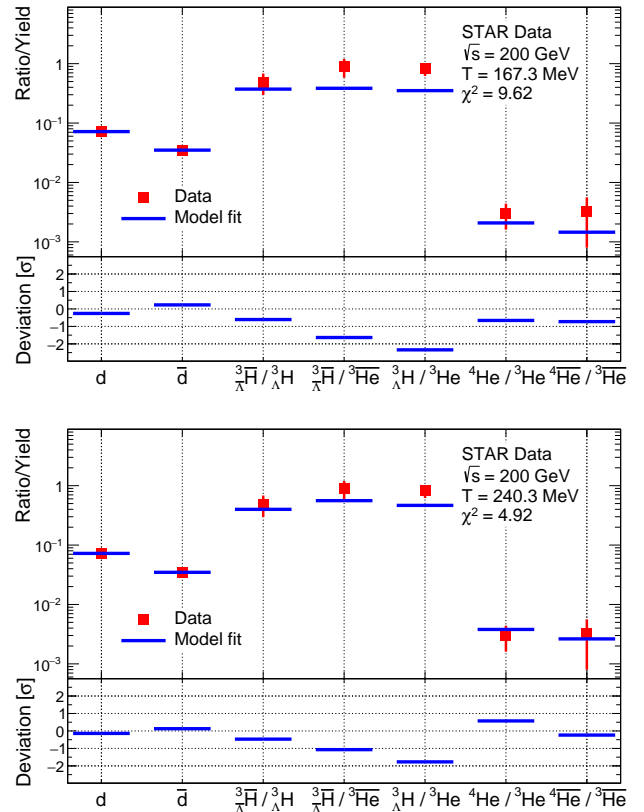


Fig. 4. Upper panel: Yield of (anti)deuteron and ratios of yields of light (anti)nuclei measured at $\sqrt{s_{NN}} = 200 \text{ GeV}$ (symbols) vs. the results of IST EoS (bars) (30), (33) (for more details see the text). The temperatures $T_A = T_h = 167.28 \pm 3.93 \text{ MeV}$ are for the single CFO with IST EoS. Insertion shows the deviation of theory from data in the units of experimental error. **Lower panel:** Same as in the upper panel, but for the separate CFO with IST EoS for $T_A = 240.29 \pm 21.38 \text{ MeV}$.

It is necessary to point out that the lower quality of the description of STAR data is generated by the ratios $\frac{3\bar{H}}{3\bar{H}e}$ and $\frac{3H}{3He}$ (see Fig. 4). This is an old puzzle [93,94] which still awaits for its solution. It is clear, however, that an increase of the CFO temperature above 175-180 MeV is not a viable solution and hence one has to look for another explanation.

The most intriguing question of this work is: how can one interpret the common CFO volume of light (anti)nuclei V_A^{com} ? Of course, at the present stage of research, this question cannot be answered with confidence, since neither the mechanism of light nuclei production nor the mechanism of their thermalization are well established. However, our educated guess is that the thermal production of light (anti)nuclei is most naturally caused by the hadronization of quark-gluon bags [60,95] formed in A+A collisions which have the Hagedorn mass spectrum [55]. Since the Hagedorn mass spectrum is a perfect thermostat and a perfect particle reservoir [96] any particle or cluster emitted by the bags with such a mass spectrum will be produced in full chemical and thermal equilibrium with the emitting bag. Such a hypothesis is not only able, in prin-

Description	T_h , MeV	T_A , MeV	μ_B^h , MeV	μ_B^A , MeV	V_A , fm ³	χ^2/dof
Single CFO, BMR	167.16 ± 3.87	167.16 ± 3.87	29.99 ± 3.25	29.99 ± 3.25	1692 ± 364	1.429
Single CFO, IST	167.28 ± 3.93	167.28 ± 3.93	30.05 ± 3.26	30.05 ± 3.26	2155 ± 411	1.482
Separate CFO, BMR	166.51 ± 4.07	178.62 ± 14.63	28.84 ± 5.37	32.63 ± 4.94	979 ± 605	1.607
Separate CFO, IST	166.51 ± 4.07	240.29 ± 21.38	28.84 ± 5.37	44.08 ± 6.81	545 ± 537	1.330

Table 3. The results obtained by the advanced HRGM for the fit of STAR data measured at $\sqrt{s} = 200$ GeV. The CFO temperature of hadrons (nuclei) is T_h (T_A), the CFO baryonic chemical potential of hadrons (nuclei) is μ_B^h (μ_B^A), while the CFO volume of nuclei is V_A . The last column gives the fit quality.

ciple, to explain the fact that the light nuclear clusters appear in full chemical and thermal equilibrium, but also the fact that the CFO temperatures extracted here from the ALICE and STAR data coincide. Moreover, in a recent preprint [97] based on a simplified transport model which, nevertheless, accurately takes into account the microscopic reactions between hadrons and heavy resonances with the Hagedorn mass spectrum it is shown that such an approach is able to reasonably well reproduce the ALICE data on hadronic and light nuclei multiplicities [45, 46, 47] with the common CFO temperature of hadrons and nuclei $T_{com} = 149$ MeV for the Hagedorn temperature $T_H = 167$ MeV. Note that this value of T_{com} almost coincides with the result $T_h = T_A = 150.35 \pm 1.91$ MeV obtained within a single CFO scenario for the ALICE data (see Table 2). Unfortunately, the authors of Ref. [97] have not analyzed the case of different CFO temperatures for hadrons and light nuclei, but the results obtained in the present work clearly demonstrate that this scenario is more favorable.

Therefore, in accordance with our hypothesis, the found values of V_A^{com} can be considered as the total volume of all quark-gluon bags from which the light (anti)nuclei are produced. If this is the case, we can predict that the entropy of quark-gluon bags produced at the collision energies $\sqrt{s_{NN}} = 2.76$ TeV and $\sqrt{s_{NN}} = 200$ GeV are related to each other as

$$\frac{S_{ALICE}}{S_{STAR}} \simeq \frac{V_A^{com} \cdot (T_A^{com})^3|_{ALICE}}{V_A^{com} \cdot (T_A^{com})^3|_{STAR}} \simeq 1.609. \quad (48)$$

Since during the hydrodynamic expansion of a perfect fluid the entropy is approximately conserved, the ratio of entropies at CFO of nuclei should be equal to the ratio of initial entropies formed at the moment of thermalization of quark-gluon bags. Therefore, the relation between initial entropies (48) can be either verified by the hydrodynamic simulations or, alternatively, it can help to fix the value of initial energy density which is used in the integrated Hydro Kinetic Model [98].

In fact, the common CFO volumes obtained for two different energies of collision allow us to determine the number of emitting sources of nuclei. From the ratio of two common CFO volumes $\frac{V(T_A^{com})|_{ALICE}}{V(T_A^{com})|_{STAR}} = 1.4015 \simeq \frac{7}{5} = \frac{14}{10}$ one can find the radius of emitting source $R_A^{source} \simeq 4.49$ fm for the number of 7 sources for the ALICE data and 5 sources for STAR data, or $R_A^{source} \simeq 3.566$ fm for the number of 14 sources for the ALICE data and 10 sources

for the STAR data. Of course, it may be just a coincidence, but the radius of emitting source $R_A^{source} \simeq 3.566$ fm is just 0.25 percent smaller than the coalescence model parameter $\delta r = 3.575$ fm used in Ref. [99] to model the formation process of light (anti)nuclei. Therefore, according to our hypothesis that the light (anti)nuclei are produced from the quark-gluon bags with Hagedorn mass spectrum at the moment of their hadronization the radius of the emitting source $R_A^{source} \simeq 3.566$ fm is, most likely, the radius of such bags. However, an additional verification of the found emitting source radius is necessary.

4 Conclusions

In this work, we suggested and exploited an entirely new strategy to elucidate the CFO parameters of light (anti)nuclei produced in A+A collisions of high energy, in which the medium of secondary hadrons is dominated by pions. This strategy is based on two different approaches to model the hard-core repulsion between light nuclei and hadrons. The first approach is based on an approximate treatment of equivalent hard-core radius of roomy nuclear clusters and pions. The second approach is rigorously derived here using a self-consistent treatment of classical excluded volumes of light nuclei and hadrons. In other words, here we generalized the induced surface tension concept to the mixtures of hadrons of different hard-core radii and light (anti)nuclei of different sizes and masses, and derived the corresponding equation of state.

Since in the pion-dominated hadronic medium both approaches should give the same results by construction, we employed such a strategy to determine the simultaneous (common) description of the same experimental data by two different approaches. In all scenarios of CFO studied here we, indeed, always found the region where these two approaches provide a simultaneous and good description of the data. Such a strategy allows us to get rid of the existing ambiguity in the light (anti)nuclei data description and to determine the CFO parameters of nuclei in A+A collisions of high energy with high confidence. In particular, for the ALICE data measured at $\sqrt{s_{NN}} = 2.76$ TeV we found that the separate CFO of nuclei provides a very high accuracy in the description of hadronic multiplicity ratios and the light (anti)nuclei yields using only 3 fitting parameters with $\chi_{tot}^2/dof \simeq 0.758$. The found CFO temperature of nuclei is $T_A^{com} = 175.1_{-3.9}^{+2.3}$ MeV and their

CFO volume is $V_A^{com} = 2660_{-1160}^{+1010}$ fm³, while the CFO of hadrons occurs at essentially lower temperature.

On the contrary, from the analysis of the STAR data measured at $\sqrt{s_{NN}} = 200$ GeV, we found that the single CFO of hadrons and nuclei with 3 fitting parameters provides a better description which, in addition, is internally self-consistent. In this case the best description of the STAR data is achieved for the following CFO parameters of nuclei: $T_A^{com} = T_h = 167.2 \pm 3.9$ MeV, $V_A^{com} = 1898.5 \pm 157.5$ fm³ and $\chi_{tot}^2/dof \simeq 1.45$.

Based on the idea that the light (anti)nuclei are produced from the quark-gluon bags with an exponential mass spectrum, we interpret the found CFO volumes of nuclei as the sum of volumes of quark-gluon bags. From this interpretation, we estimated the ratio of initial entropy of thermalized bags for A+A collision energies $\sqrt{s_{NN}} = 200$ GeV and $\sqrt{s_{NN}} = 2.76$ TeV and the number of the emitting sources of nuclei, which, in principle, can be verified by the hydrodynamic or hydro-kinetic approaches. Surprisingly, if the number of such sources is 14 for the ALICE energy and, consequently, 10 for the STAR energy, as it is required by their common CFO volumes, then the radius of emitting sources of nuclei is 3.566 fm, which practically coincides with the value of the coalescence distance used in a successful transport code simulating the production of nuclei [99].

In the present work we demonstrate that the experimental data for the yields of hadrons and light nuclei produced in heavy-ion collisions at RHIC and LHC energies can be described with a very high accuracy, if one uses a formulation of the HRGM that employs the classical second virial coefficients corresponding to a hard-sphere model of nuclei and hadrons. At the same time it is shown that the determination of the CFO temperature of light nuclei is a rather delicate issue since the result depends on the underlying scenario of their CFO.

The simple model of hard spheres for the repulsive interactions between hadrons and nuclei as employed in the present work can of course only be considered as an intermediate step in our understanding of the formation of hadrons and light nuclei from a hadronizing quark-gluon plasma. Microphysical approaches should be further developed which treat hadrons and nuclei as multi-quark clusters and would allow for a deeper understanding of the hadrochemistry on the quark level. One aspect of a description on this level would be the explanation of the short-range repulsion by quark Pauli blocking among hadrons (see, e.g., Ref. [3]), eventually augmented by repulsive multi-pomeron exchange forces that have proven essential to describe large-angle nucleus-nucleus scattering at the Fermi energy and in resolving the hyperon puzzle of neutron star structure [100]. From the further systematic analysis of light nuclei production measured in the heavy ion collision experiments a picture may emerge in which the puzzling result of a high CFO temperature finds its explanation by a hadronization of multi-quark states from the QGP, as it was already anticipated in Ref. [95] and emphasized again in Ref. [59] in the light of the recent

experiments.

Author contributions. K.A.B. developed the idea behind this work and together with D.B.B. took the lead in writing the manuscript. O.V.V., B.E.G., V.V.S. and E.S.Z. performed fit of the experimental data on the light (anti)nuclei and hadrons. O.I.I., N.S.Y. and E.G.N. verified the analytical methods. Both N.S.Y. and S.V.K., helped in calculating the CFO volume of hadrons and designed the figures. G.M.Z., L.V.B., E.E.Z., S.K., G.R.F. and A.V.T. contributed to the interpretation of the results and provided a critical feedback. All authors discussed the results and contributed to the final manuscript.

Acknowledgments. The authors are thankful to Dmytro Oliinychenko for bringing to our attention Ref. [44] and for illuminating discussions, and to Grigory Nigmatkulov and Ivan Yakimenko for the valuable comments. K.A.B. and G.M.Z. acknowledge support from the NAS of Ukraine by its priority project “Fundamental properties of the matter in the relativistic collisions of nuclei and in the early Universe” (No. 0120U100935). V.V.S. and O.I.I. are thankful for the support by the Fundação para a Ciência e Tecnologia (FCT), Portugal, by the project UID/04564/2020. The work of O.I.I. was supported by the project CENTRO-01-0145-FEDER-000014 via the CENTRO 2020 program, and POCI-01-0145-FEDER-029912 with financial support from POCI, in its FEDER component and by the FCT/MCTES budget via national funds (OE). The work of L.V.B. and E.E.Z. was supported by the Norwegian Research Council (NFR) under grant No. 255253/ F53 CERN Heavy Ion Theory, and by the RFBR grants 18-02-40085 and 18-02-40084. K.A.B., O.V.V., N.S.Ya. and L.V.B. thank the Norwegian Agency for International Cooperation and Quality Enhancement in Higher Education for the financial support under grants CPEA-LT-2016/10094 and UTF-2016-long-term/10076. A.V.T. acknowledges partial support from RFBR under grant No. 18-02-40086 and from the Ministry of Science and Higher Education of the Russian Federation, Project “Fundamental properties of elementary particles and cosmology” No 0723-2020-0041. D.B.B. received funding from the RFBR under grant No. 18-02-40137. D.B.B. and A.V.T. acknowledge a partial support from the National Research Nuclear University “MEPhI” in the framework of the Russian Academic Excellence Project (contract no. 02.a03.21.0005, 27. 08.2013). The authors are grateful to the COST Action CA15213 “THOR” for supporting their networking.

References

1. W. Ebeling, D. Blaschke, R. Redmer, H. Reinholz and G. Röpke, *J. Phys. A* **42**, 214033 (2009).
2. G. Röpke, D. Blaschke, T. Döppner, C. Lin, W. D. Kraeft, R. Redmer and H. Reinholz, *Phys. Rev. E* **99**, no. 3, 033201 (2019).
3. D. Blaschke, H. Grigorian and G. Röpke, *Particles* **3**, no.2, 477-499 (2020).

4. S. Typel, G. Röpke, T. Klähn, D. Blaschke and H. H. Wolter, *Phys. Rev. C* **81**, 015803 (2010).
5. M. Hempel, K. Hagel, J. Natowitz, G. Röpke and S. Typel, *Phys. Rev. C* **91**, no. 4, 045805 (2015).
6. G. Röpke, *Phys. Rev. C* **101**, no.6, 064310 (2020).
7. J. M. Lattimer and F. D. Swesty, *Nucl. Phys. A* **535**, 331 (1991).
8. H. Shen, H. Toki, K. Oyamatsu and K. Sumiyoshi, *Nucl. Phys. A* **637**, 435 (1998).
9. M. Hempel, J. Schaffner-Bielich, S. Typel and G. Röpke, *Phys. Rev. C* **84**, 055804 (2011).
10. G. Röpke, N.-U. Bastian, D. Blaschke, T. Klähn, S. Typel and H. H. Wolter, *Nucl. Phys. A* **897**, 70 (2013); [arXiv:1209.0212 [nucl-th]].
11. N. U. F. Bastian, D. Blaschke, T. Fischer and G. Röpke, *Universe* **4**, 67 (2018) and references therein.
12. S. Mrowczynski, *Acta Phys. Polon. B* **48**, 707 (2017).
13. K. J. Sun, L. W. Chen, C. M. Ko and Z. Xu, *Phys. Lett. B* **774**, 103-107 (2017).
14. K. J. Sun, L. W. Chen, C. M. Ko, J. Pu and Z. Xu, *Phys. Lett. B* **781**, 499-504 (2018).
15. K. J. Sun, C. M. Ko and B. Dönigus, *Phys. Lett. B* **792**, 132-137 (2019).
16. V. Vovchenko, B. Dönigus and H. Stoecker, *Phys. Lett. B* **785**, 171-174 (2018).
17. F. Bellini and A. P. Kalweit, *Phys. Rev. C* **99**, no.5, 054905 (2019).
18. F. Bellini, K. Blum, A. P. Kalweit and M. Puccio, [arXiv:2007.01750 [nucl-th]].
19. Y. Cai, T. D. Cohen, B. A. Gelman and Y. Yamauchi, *Phys. Rev. C* **100**, no.2, 024911 (2019).
20. J. Aichelin, E. Bratkovskaya, A. Le Fèvre, V. Kireyeu, V. Kolesnikov, Y. Leifels, V. Voronyuk and G. Coci, *Phys. Rev. C* **101**, no.4, 044905 (2020).
21. D. Oliinychenko, talk given at XXVIIIth Conference “Quark Matter 2019“, arXiv:2003.05476v1 [hep-ph] and references therein.
22. S. Mrowczynski, arXiv:2004.07029v1 [nucl-th] and references therein.
23. D. Blaschke, A. V. Friesen, Y. B. Ivanov, Y. L. Kalinovsky, M. Kozhevnikova, S. Liebing, A. Radzhabov and G. Röpke, arXiv:2004.01159 [hep-ph].
24. D. Blaschke, G. Röpke, Y. Ivanov, M. Kozhevnikova and S. Liebing, *Springer Proc. Phys.* **250**, 183 (2020).
25. D. R. Oliinychenko, K. A. Bugaev and A. S. Sorin, *Ukr. J. Phys.* **58**, 211 (2013).
26. K. A. Bugaev, D. R. Oliinychenko, A. S. Sorin and G. M. Zinovjev, *Eur. Phys. J. A* **49**, 30 (2013).
27. K. A. Bugaev *et al.*, *Europhys. Lett.* **104**, (2013) 22002.
28. K. A. Bugaev, A. I. Ivanytskyi, D. R. Oliinychenko, E. G. Nikonov, V. V. Sagun and G. M. Zinovjev, *Ukr. J. Phys.* **60**, 181 (2015).
29. V. V. Sagun, *Ukr. J. Phys.* **59**, 755 (2014).
30. K. A. Bugaev *et al.*, *Phys. Part. Nucl. Lett.* **12**, 238 (2015).
31. K. A. Bugaev *et al.*, *Eur. Phys. J. A* **52**, 175 (2016).
32. K. A. Bugaev *et al.*, *Eur. Phys. J. A* **52**, 227 (2016).
33. K. A. Bugaev *et al.*, *Phys. Part. Nucl. Lett.* **15**, 210 (2018).
34. K. A. Bugaev *et al.*, *EPJ Web of Conferences* **204**, 03001 (2019).
35. A. Andronic, P. Braun-Munzinger and J. Stachel, *Nucl. Phys. A* **772**, 167 (2006) and references therein.
36. V. V. Sagun, A. I. Ivanytskyi, K. A. Bugaev and I. N. Mishustin, *Nucl. Phys. A* **924**, 24 (2014).
37. V. V. Sagun *et al.*, *Eur. Phys. J. A* **54**, 100 (2018).
38. K. A. Bugaev *et al.*, *Nucl. Phys. A* **970**, 133 (2018).
39. K. A. Bugaev, *Eur. Phys. J. A* **55**, 215 (2019).
40. N. S. Yakovenko, K. A. Bugaev, L.V. Bravina and E. E. Zabrodin, arXiv:1910.04889 [nucl-th] p. 1-13.
41. S. Bazak and S. Mrowczynski, *Eur. Phys. J. A* **56**, no.7, 193 (2020).
42. STAR Collaboration (B. I. Abelev *et al.*), *Science* **328**, No 5974, p. 58-62 (2010).
43. STAR Collaboration (H. Agakishiev *et al.*), *Nature* **473**, No 7347, p. 353-356 (2011).
44. STAR Collaboration (J. Adam *et al.*), *Phys. Rev. C* **99**, 064905 (2019).
45. ALICE Collaboration (J. Adam *et al.*), *Phys. Rev. C* **93**, 024917 (2016).
46. ALICE Collaboration (L. Ramona *et al.*), *AIP Conf. Proc.* **1701**, (1) 080009 (2016).
47. ALICE Collaboration (J. Adam *et al.*), *Phys. Lett. B* **754**, 360 (2016).
48. R. Venugopalan and M. Prakash, *Nucl. Phys. A* **546**, 718 (1992).
49. E. Shuryak and J. M. Torres-Rincon, *Phys. Rev. C* **100**, 024903 (2019) and references therein.
50. E. Shuryak and J. M. Torres-Rincon, *Phys. Rev. C* **101**, no.3, 034914 (2020).
51. L. M. Satarov, M. N. Dmitriev and I. N. Mishustin, *Phys. Atom. Nucl.* **72**, 1390 (2009).
52. K. A. Bugaev, A. I. Ivanytskyi, V. V. Sagun, E. G. Nikonov and G. M. Zinovjev, *Ukr. J. Phys.* **63**, 863 (2018) and references therein
53. K. A. Bugaev, *Nucl. Phys. A* **606**, 559 (1996).
54. K. A. Bugaev, *Phys. Rev. Lett.* **90**, 252301 (2003) and references therein
55. R. Hagedorn, *Nuovo Cim. Suppl.* **3**, 147 (1965).
56. S. Chatterjee *et al.*, *Adv. High Energy Phys.* 2015, 349013 (2015) and references therein.
57. J. Cleymans, S. Kabana, I. Kraus, H. Oeschler, K. Redlich and N. Sharma, *Phys. Rev. C* **84** 054916 (2011).
58. J. Stachel, A. Andronic, P. Braun-Munzinger and K. Redlich, *J. Phys. Conf. Ser.* **509**, 012019 (2014).
59. A. Andronic, P. Braun-Munzinger, K. Redlich and J. Stachel, *Nature* **561**, no.7723, 321-330 (2018).
60. K. A. Bugaev *et al.*, *J. of Phys. Conf. Series* **1390**, 012038 (2019).
61. P. Braun-Munzinger and B. Dönigus, *Nucl. Phys. A* **987**, 144 (2019) and references therein.
62. B. E. Grinyuk *et al.*, arXiv:2004.05481v1 [hep-ph] (2020).
63. A. Bohr and B. Mottelson, *Nuclear Structure*, vol. 1 (Benjamin, New York, 1969).
64. I. Angeli and K. Marinova, *At. Data Nucl. Data Tables* **99**, 69 (2013).
65. H. Nemura, Y. Suzuki, Y. Fujiwara, C. Nakamoto, *Prog. Theor. Phys.* **103**, 929 (2000); arXiv:nucl-th/9912065.
66. J. Rafelski, *Phys. Lett. B* **62**, 333 (1991).
67. E. Beth and G. Uhlenbeck, *Physica* **4**, 915 (1937).
68. J. Hüfner, S. P. Klevansky, P. Zhuang and H. Voss, *Annals Phys.* **234**, 225 (1994).
69. A. Wergieluk, D. Blaschke, Y. L. Kalinovsky and A. Friesen, *Phys. Part. Nucl. Lett.* **10**, 660 (2013).
70. D. Blaschke, M. Buballa, A. Dubinin, G. Röpke and D. Zablocki, *Annals Phys.* **348**, 228 (2014).
71. D. Blaschke, A. Dubinin, A. Radzhabov and A. Wergieluk, *Phys. Rev. D* **96**, no. 9, 094008 (2017).

72. D. Blaschke, A. Dubinin and L. Turko, arXiv:1611.09845v2 [hep-ph].
73. D. Blaschke, A. Dubinin and L. Turko, *Acta Phys. Polon. Supp.* **10**, 473 (2017).
74. G. Baym, *Phys. Rev.* **127**, 1391 (1962).
75. B. Vanderheyden and G. Baym, *J. Stat. Phys.* **93**, 843 (1998).
76. K. A. Bugaev and P. T. Reuter, *Ukr. J. Phys.* **52**, 489 (2007) and references therein.
77. K. Huang, *Statistical Mechanics* (Wiley & Sons, New York, 1967).
78. L. M. Satarov, K. A. Bugaev, I. N. Mishustin, *Phys. Rev. C* **91**, 055203 (2015).
79. V. Vovchenko, H. Stöcker, *J. Phys. G* **44**, 055103 (2017).
80. J. P. Hansen and I. R. McDonald, *Theory of Simple Fluids* (Academic Press, Amsterdam, 2006).
81. A. Chodos, R. L. Jaffe, K. Johnson, C. B. Thorn, V. F. Weisskopf, *Phys. Rev. D* **9**, 3471 (1974).
82. B. Abelev *et al.* [ALICE Collaboration], *Phys. Rev. C* **88** (2013) 044910.
83. B. B. Abelev *et al.* [ALICE Collaboration], *Phys. Lett. B* **728** (2014) 216; Erratum: [*Phys. Lett. B* **734** (2014) 409].
84. B. B. Abelev *et al.* [ALICE Collaboration], *Phys. Rev. Lett.* **111** (2013) 222301.
85. B. B. Abelev *et al.* [ALICE Collaboration], *Phys. Rev. C* **91** (2015) 024609.
86. A. Andronic, P. Braun-Munzinger, K. Redlich and J. Stachel, *J. Phys. Conf. Ser.* **779**, 012012 (2017).
87. Wuppertal-Budapest Collaboration (S. Borsanyi *et al.*), *JHEP* **1009**, 073 (2010).
88. HotQCD Collaboration (A. Bazavov *et al.*), *Phys. Rev. D* **90**, 094503 (2014).
89. A. Bazavov *et al.* [HotQCD], *Phys. Lett. B* **795** (2019), 15-21.
90. J. Adams *et al.*, *Phys. Rev. Lett.* **92**, 112301 (2004).
91. J. Adams *et al.*, *Phys. Lett. B* **612**, 181 (2005).
92. A. Billmeier *et al.*, *J. Phys. G* **30**, S363 (2004).
93. A. Andronic, P. Braun-Munzinger, J. Stachel and H. Stoecker, *Phys. Lett. B* **697**, 203 (2011).
94. X. Xu and R. Rapp, *Eur. Phys. J. A* **55**, 68 (2019); arXiv:1809.04024v2 [nucl-th] and references therein.
95. G. F. Chapline and A. K. Kerman, MIT-CTP-695 (1978).
96. L. G. Moretto, K. A. Bugaev, J. B. Elliott and L. Phair, *Europhys. Lett.* **76**, 402 (2006); LBNL preprint 56898.
97. K. Gallmeister and C. Greiner, [arXiv:2007.08258 [hep-ph]].
98. V. Yu. Naboka, Iu. A. Karpenko and Yu. M. Sinyukov, *Phys. Rev. C* **93**, 024902 (2016).
99. S. Sombun *et al.*, *Phys. Rev. C* **99**, 014901 (2019).
100. Y. Yamamoto, T. Furumoto, N. Yasutake and T. A. Rijken, *Eur. Phys. J. A* **52**, no.2, 19 (2016).